ACCSCIENCE PUBLISHING

Eurasian Journal of Medicine and Oncology

ORIGINAL RESEARCH ARTICLE

Autophagy-related-gene signature predicts survival outcomes and the tumor immune landscape in skin cutaneous melanoma

Yadong Xue[1,2], Yunjin Xie[2,3,4,5,6], Xiyuan Zhang[2,3,4,5,6]*, and Mingzhu Yin[2,3,4,5,6]*

[1]Dermatology Department, The First Affiliated Hospital of Harbin Medical University, Harbin, Heilongjiang, China

[2]Clinical Research Center, Medical Pathology Center, Cancer Early Detection and Treatment Center, and Translational Medicine Research Center, Chongqing University Three Gorges Hospital, Chongqing University, Chongqing, China

[3]Chongqing Technical Innovation Center for Quality Evaluation and Identification of Authentic Medicinal Herbs, Chongqing, China

[4]Chongqing University Three Gorges Hospital and Academy for Advanced Interdisciplinary Technology, Chongqing University Ferenc Krausz Nobel Laureate Scientific Workstation, Chongqing, China

[5]School of Medicine, Chongqing University, Chongqing, China

[6]Institute of Advanced Interdisciplinary Studies, Chongqing University, Chongqing, China

***Corresponding authors:**
Mingzhu Yin (yinmingzhu@cqu.edu.cn);
Xiyuan Zhang (202537109683@stu.cqu.edu.cncqu.edu.cn)

Citation: Xue Y, Xie Y, Zhang X, Yin M. Autophagy-related-gene signature predicts survival outcomes and the tumor immune landscape in skin cutaneous melanoma. *Eurasian J Med Oncol*. 2026;10(5):025370399. doi: 10.36922/EJMO025370399

Received: September 14, 2025

Revised: November 5, 2025

Accepted: December 2, 2025

Published online: August 12, 2026

Copyright: © 2026 Author(s). This is an Open-Access article distributed under the terms of the Creative Commons Attribution License, permitting distribution, and reproduction in any medium, provided the original work is properly cited.

Publisher's Note: AccScience Publishing remains neutral with regard to jurisdictional claims in published maps and institutional affiliations.

Abstract

Introduction: Skin cutaneous melanoma (SKCM) is a malignant skin cancer characterized by heterogeneous outcomes. Autophagy exerts dual effects on tumor progression and immune modulation.

Objective: This study aims to investigate whether autophagy-related genes can stratify melanoma patients with different prognoses and to examine their association with the immune microenvironment.

Methods: We identified 371 autophagy-related genes from the Human Autophagy Database and analyzed transcriptomic and clinical data from 405 SKCM cases from The Cancer Genome Atlas (TCGA). An autophagy-based prognostic signature was initially screened by univariate Cox regression and then refined using Least Absolute Shrinkage and Selection Operator Cox regression. Risk scores derived from this signature classified patients into high- and low-risk groups, and the predictive power of the signature was validated in TCGA and Gene Expression Omnibus datasets. Functional enrichment, differential expression, and immune deconvolution analyses (Cell-type Identification by Estimating Relative Subsets of Known RNA Transcripts) were used to explore molecular and immune differences between groups.

Results: We constructed a 102-autophagy-related-gene signature, which robustly stratifies patients with distinct survival outcomes in different cohorts. Low-risk tumors exhibited immune-activating transcriptional programs and higher infiltration of cluster of differentiation (CD)8^+ T lymphocytes, natural killer cells, plasma cells, and memory $CD4^+$ T lymphocytes. High-risk tumors were associated with oncogenic signaling pathways and immunosuppressive subsets, such as M2 macrophages and Tregs. Canonical immune checkpoints, including *PDCD1*, *CD274*, *CTLA4*, *LAG3*, and *TIGIT*, were upregulated in the low-risk group and correlated significantly with effector immune infiltration, presenting an "immune-inflamed" phenotype.

Conclusion: This autophagy-related-gene signature distinguished prognostic subgroups and highlighted biological and immune diversity in melanoma, providing potential directions for future autophagy research.

Keywords: Skin cutaneous melanoma; Autophagy; Immune microenvironment; Prognostic signature; Checkpoint blockade

1. Introduction

Melanoma is a lethal skin cancer that derives from melanocytes, accounting for nearly three-quarters of all deaths from skin cancers worldwide.[1,2] Its incidence continues to increase, especially among fair-skinned populations with chronic ultraviolet exposure, which induces DNA damage and drives mutations in oncogenes, such as *BRAF* and *NRAS*.[3,4] Advanced melanoma is characterized by rapid dissemination and unfavorable prognosis, imposing a substantial burden on healthcare systems.[1,4,5] Recent breakthroughs in molecular targeted agents (such as *BRAF* inhibitors) and immunotherapies (such as immune checkpoint inhibitors) have conferred significant survival benefits to patients, but responses to these therapies are highly heterogeneous, and some patients may fail to respond or develop acquired resistance.[6,7] Consequently, identifying reliable molecular biomarkers to predict prognosis and treatment outcomes has become an urgent clinical need. Previous clinical factors, such as tumor stage and Breslow thickness, cannot fully account for melanoma's molecular complexity.[8] Therefore, integrative genomic models that combine molecular features to better explain clinical phenotypes and predict risk would be beneficial for personalized treatment.

Autophagy is a well-conserved intracellular degradation and recycling process that exerts dual and context-dependent effects in cancer.[9] During early tumor development, autophagy can maintain cell homeostasis and reduce genomic instability, potentially suppressing tumor formation.[10,11] Once tumors are established, tumor cells exploit autophagy to survive under stress, promote metabolic adaptation, and escape from immune attack.[12] In recent years, researchers found that autophagy was involved in the tumor progression, metastatic capacity, and therapy resistance of melanoma[13], suggesting that autophagy-related transcriptional programs may hold prognostic and therapeutic relevance.

Recently, several autophagy-related prognostic models have been constructed in melanoma, and all have demonstrated independent prognostic value for overall survival (OS).[14–16] However, most existing models primarily focus on survival prediction and have paid limited attention to the immune microenvironment, despite growing evidence showing that autophagy interacts closely with tumor immunity.[17] Building on these foundations, our study integrates a comprehensive analysis of both autophagy-related genes and immune characteristics, providing a deeper understanding of the biological programs underlying risk stratification and suggesting possible links between autophagy and immune responsiveness.

In this study, we identified a set of autophagy-associated genes and applied Cox regression to identify the relevant prognostic genes within The Cancer Genome Atlas (TCGA)-skin cutaneous melanoma (SKCM) cohort. After selecting these genes, we validated the model across multiple independent Gene Expression Omnibus (GEO) datasets to ensure its stability and generalizability, confirming that the risk score derived from the prognostic signature retains predictive power across various patient populations. Beyond survival prediction, we examined the distinct molecular and phenotypic features of the high- and low-risk groups using functional enrichment and immune deconvolution analyses. Our results demonstrate that the signature captures distinct immune features, suggesting its potential to reveal key insights into the relationship between autophagy and tumor immunity in melanoma.

Overall, our study establishes a reliable autophagy-related-gene signature that reflects both prognostic and immune features of melanoma, offering a resource for future research on autophagy-based immunotherapy.

2. Materials and methods

2.1. Data sources and autophagy gene collection

The gene set comprising 371 autophagy-related genes was sourced from the Human Autophagy Database.[18] Transcriptomic sequencing data and matched clinical information from SKCM cases were extracted from the TCGA-SKCM resource through the University of California, Santa Cruz Xena portal to serve as an internal cohort. To validate the robustness of our findings in the internal dataset, independent datasets (GSE215119,

GSE190113, GSE65904, and GSE91061) were accessed via the GEO repository for external validations.

2.2. Data preprocessing and cohort partitioning

In the TCGA-SKCM cohort, we removed samples lacking complete clinical information or OS data. The remaining RNA sequencing data were originally in fragments per kilobase of transcript per million mapped reads (FPKM) format. We transformed these values into $\log_2$(FPKM + 1) to normalize skewed expression distributions, yielding 405 tumor samples for analysis.

External datasets underwent appropriate preprocessing based on their platform types. The microarray dataset (GSE65904) was processed by mapping probe IDs to official gene symbols according to platform annotations. When several probes mapped to the same gene, we used the mean signal intensity of these probes as the final expression level. For the three RNA-seq datasets, including GSE190113, GSE215119, and GSE91061, which provided gene-level read counts, we converted the expression values into transcripts per million to control sequencing depth and gene length. All validation datasets were then log2-transformed. To ensure datasets from different platforms were comparable, we used *z*-score normalization within each cohort. This step reduced the influence of batch effects and allowed us to focus on relative gene expression patterns rather than absolute expression values.

We randomly allocated patients to a training set (70%, $n = 283$) and a test set (30%, $n = 122$), ensuring balanced distributions of clinical variables. The training set was utilized to establish a model and select parameters, while the test set and external GEO datasets were used to evaluate the stability and general performance of the signature.

2.3. Cox regression analysis

To explore the association between autophagy-related genes and patient outcomes, we first performed univariate Cox regression on the training set. Each gene in the gene set ($n = 371$) was assessed individually for its association with OS. The genes with a significant association with OS (p-value < 0.05) were retained as candidate genes ($n = 140$) for subsequent modeling. The analysis was performed in R software (v4.2.1, R Foundation for Statistical Computing, Austria) using the survival package. To reduce feature redundancy and prevent overfitting, we next applied the Least Absolute Shrinkage and Selection Operator (LASSO) Cox regression model on the training set to select prognostic genes. The analyses were conducted using the R package glmnet with 5-fold cross-validation to select the optimal penalty parameter. The model with the lowest lambda value (lambda.min) was selected as the final model, yielding a prognostic signature consisting of 102 genes. Non-zero coefficients were extracted using the *coef* function in glmnet.

2.4. Risk score calculation and patient stratification

For each patient, we computed the risk score as follows (**Equation [1]**):

$$Risk\ score = \sum_{j=1}^{n} \beta_j \times Expression_j \quad (1)$$

where β_j stands for the regression coefficient of gene j from the LASSO Cox model, and $Expression_j$ is the normalized expression level of gene j. Patients in each dataset (i.e., the internal TCGA set and the external GEO sets) were divided into high- or low-risk groups based on the cohort-specific median risk score.

2.5. Survival analysis and multivariate Cox regression

We assessed differences in OS between risk groups using Kaplan–Meier (KM) survival curves, calculated via the *survfit* function in the R package survival. Survival differences between groups were evaluated by the log-rank test. Survival curves were visualized using the *ggsurvplot* function from the survminer package, allowing clear comparison of long-term survival trends.

To evaluate the independence of the autophagy-related-gene signature from clinical variables, multivariate Cox regression was performed incorporating risk score, age, gender, and tumor stage. Tumor stage was dichotomized into early (stage 0, I, and II) and late (stage III–IV). Hazard ratios, 95% confidence intervals, and p-values were derived with the Wald test. The Benjamini–Hochberg false discovery rate (FDR) method was utilized to correct for multiple comparisons. The forest plot was generated with the *ggforest* function in the R package survminer.

2.6. Differential expression analysis

To identify transcriptional alterations associated with the autophagy-related prognostic signature, patients in the TCGA training set were assigned to the high- or low-risk groups based on the median risk score. Differential expression analysis was performed using the R package limma to identify differentially expressed genes (DEGs). Genes with an FDR-corrected p-value < 0.05 (Benjamini–Hochberg correction) and an absolute $\log_2$ fold change > 1 were considered significant.

2.7. Visualization of differentially expressed genes

The overall distribution of DEGs ($n = 553$) was illustrated using a volcano plot, which highlights both the magnitude

and significance of expression differences. The top 10 upregulated genes in each group were labeled to enhance interpretability. To visualize representative transcriptional patterns, the top 50 significant DEGs (ranked by FDR-corrected *p*-value) were selected for hierarchical clustering. The heatmap was generated by the R package pheatmap to display their expression profiles across high- and low-risk groups, with rows representing genes and columns representing patients.

2.8. Functional enrichment analysis

We performed gene ontology (GO) annotation to identify the functional enrichment of DEGs. Significantly enriched biological processes (FDR-adjusted $p < 0.05$) were identified through functional enrichment analysis using the R package clusterProfiler. The results were displayed as bar plots for clear visualization.

2.9. Immune cell-infiltration analysis

We analyzed immune cell composition in each risk group by the Cell-type Identification by Estimating Relative Subsets of Known RNA Transcripts (CIBERSORT) algorithm.[19] This tool estimates the relative abundance of 22 immune cell types based on gene expression data and a reference signature matrix (LM22). CIBERSORT was run with 1,000 permutations to ensure reliable deconvolution.[20] The fractions of immune populations in each category were compared between the two risk groups by the Wilcoxon rank-sum test, regarding $p < 0.05$ as statistically significant. Visualization was performed with the R package ggplot2.

2.10. Immune pathway activity scoring via single-sample gene set enrichment analysis

To measure the activity of immune-related biological processes, we conducted single-sample gene set enrichment analysis using the *gsva()* function (method = "ssgsea") in R. Gene sets corresponding to immune pathways were retrieved from the GO database, including leukocyte-mediated immunity (GO:0002443 and GO:0002449), adaptive immune response (GO:0002250), B cell-mediated immunity (GO:0019724), leukocyte cell-cell adhesion (GO:0007159), and regulation of T cell activation (GO:0050863). Gene sets corresponding to these GO terms were retrieved from the R package org.Hs.eg.db. For each individual in the TCGA test dataset and the GSE65904 validation cohort, enrichment scores were computed, and group differences were compared using the Wilcoxon rank-sum test. Results were visualized with box plots in the R package ggplot2.

2.11. Correlation between checkpoint expression and immune infiltration

To explore associations between checkpoint expression and immune infiltration levels, Spearman correlation analysis was performed between checkpoint gene expression levels and the estimated fractions of immune cell subsets derived from CIBERSORT analysis. Spearman correlation coefficients and corresponding *p*-values were calculated using the stats package in R, and results were visualized with scatter plots generated by the R package ggplot2.

3. Results

3.1. Development and verification of a prognostic model based on autophagy-associated genes

To investigate the prognostic relevance of autophagy-related genes in SKCM, we identified 371 autophagy-related genes from the Human Autophagy Database. Transcriptomic profiles and matched clinical information of SKCM patients were sourced from the TCGA-SKCM cohort. After excluding cases with incomplete survival or clinical data, 405 patients were included in the analysis. These patients were randomized into a training set (n = 283, 70%) and a test set (n = 122, 30%) to allow independent model evaluation.

In the training set, we initially conducted univariate Cox regression to identify genes associated with OS. We identified 140 genes in total ($p < 0.05$, Figure 1A). We then applied LASSO Cox regression to further narrow down the candidate genes and built a final prognostic model composed of 102 autophagy-related genes. A risk score was calculated for each patient, and patients were stratified into two risk groups (high vs. low) based on the median risk score in the training cohort, as described in Section 2 (Materials and Methods).

According to KM analysis, high-risk patients had significantly worse OS than low-risk patients (Figure 1B). The model also exhibited independent prognostic value in the TCGA test set (Figure A1). Additionally, the model showed similar performance in three GEO datasets (GSE215119, GSE190113, and GSE65904; Figure A1B and A1C). These results indicate that the autophagy-related prognostic signature is reproducible across multiple datasets.

To further characterize the molecular features associated with risk stratification, we visualized the expression profiles of all genes included in the signature across patients in the training set (Figure 1C). Genes with negative regression

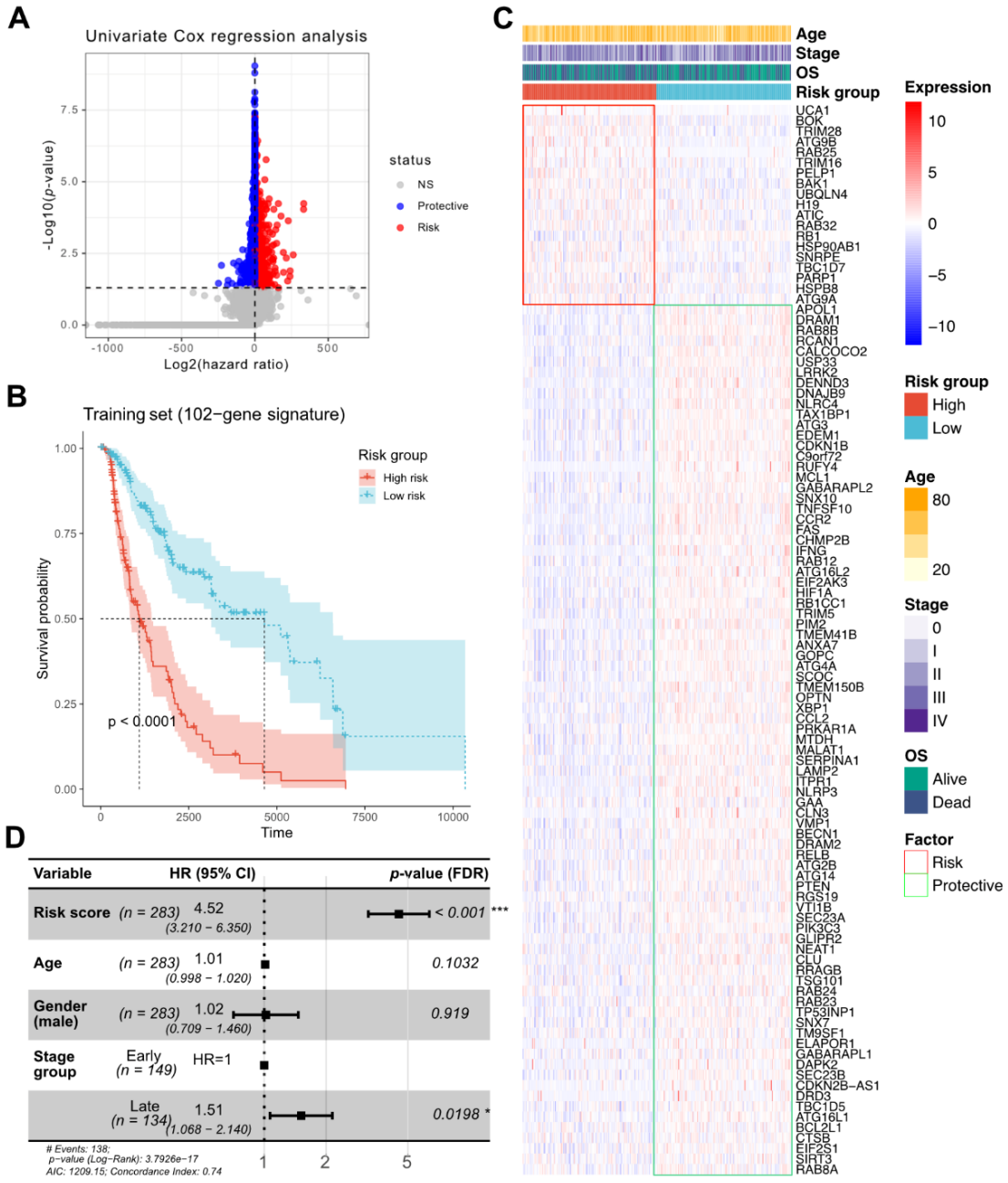


Figure 1. Construction and validation of an autophagy-related prognostic signature in skin cutaneous melanoma. (A) Volcano plot of univariate Cox regression analysis for 371 autophagy-related genes. Red dots indicate risk genes (HR > 1, $p < 0.05$), blue dots represent protective genes (HR < 1, $p < 0.05$), and grey dots denote genes without significant prognostic value ($p > 0.05$). (B) Kaplan–Meier survival curves for patients in The Cancer Genome Atlas training set stratified by the 102-gene signature risk score. (C) The heatmap shows the expression profiles of 102 Least Absolute Shrinkage and Selection Operator-selected prognostic genes in the training set. Top annotation bars indicate clinical variables, including risk group, overall survival status, stage, and age. (D) Forest plot of multivariate Cox regression analysis evaluating the independent prognostic value of the risk score alongside clinical variables (age, gender, and tumor stage). HRs and 95% CIs were derived from Cox proportional hazards models. Statistical significance was determined by the Wald test and adjusted for multiple comparisons by the Benjamini–Hochberg FDR method in D.

Notes: *$p < 0.05$; ***$p < 0.001$.

Abbreviations: CIs: Confidence intervals; FDR: False discovery rate; HR: Hazard ratio; NS: Not significant; OS: Overall survival.

coefficients tended to show higher expression in the low-risk group, reflecting their association with better outcomes. Conversely, genes linked to poorer prognosis, as indicated by positive regression coefficients, were more abundant in patients classified as high risk (Table S1). The expression patterns showed limited correlation with conventional clinical variables, suggesting that the prognostic signature provides information beyond traditional staging systems.

We next examined whether the risk score could serve as an independent prognostic factor beyond established clinical variables. To address this, we performed a multivariate Cox regression analysis that included age, gender, tumor stage (early vs. late), and the risk score. We found that the risk score remained a strong and significant predictor of OS (Figure 1D). Tumor stage also demonstrated an independent association with survival, consistent with its well-established role in melanoma outcomes.[21] In contrast, neither age nor gender showed a significant effect in the multivariate model. In total, our results show that the risk score is an independent and powerful prognostic indicator that improves patient stratification and may provide new insights for clinical prediction based on autophagy-related gene expression.

3.2. Immune landscape associated with the risk signature

To uncover the biological processes driving the prognostic separation defined by the autophagy-based signature, we compared the gene expression patterns between patients classified by risk score in the TCGA training set. Differential expression analysis identified 553 genes that were significantly altered between the two groups. The volcano plot demonstrated a predominance of upregulated genes in the low-risk group (Figure 2A), consistent with the clustering pattern of the top 50 DEGs, which showed preferential expression in low-risk tumors (Figure 2B).

Closer inspection revealed that numerous DEGs that encode immune-regulatory and interferon-stimulated factors showed increased expression in the low-risk group. For instance, *SAMD9L*, an interferon-inducible antiviral factor and tumor suppressor critical for innate immune defense, harbors germline and somatic variants associated with myeloid malignancies, including pediatric myelodysplastic syndromes/acute myeloid leukemia and monosomy-7 syndromes.[22,23] *BIRC3*, encoding cellular inhibitor of apoptosis protein 2, participates in the regulation of apoptosis and nuclear factor kappa-light-chain-enhancer of activated B cells (NF-κB) signaling and contributes to tumor cell survival and immune homeostasis.[24] Cylindromatosis (CYLD) protein, a deubiquitinase and tumor suppressor, restrains NF-κB signaling and interacts with additional pathways relevant to immune regulation.[25,26] Consistent with this role, its reduced expression is known to associate with an inferior prognosis in melanoma.[27] In our cohort, *CYLD* upregulation emerged as a defining feature of the low-risk group and underlies its favorable prognosis. *IFIH1* encodes melanoma differentiation-associated protein 5, a cytosolic viral RNA sensor, which activates type I interferon responses and downstream adaptive immunity.[28] Collectively, the upregulation of these genes in the low-risk cohort suggests the presence of a transcriptional program conducive to immune activation and enhanced antitumor surveillance.

Conversely, genes enriched in the high-risk group were mainly linked to tumor-promoting pathways and immune suppression. *RAC3*, encoding steroid receptor coactivator 3/amplified in breast cancer 1, functions as an oncogenic coactivator that enhances tumor cell proliferation and migration partly through protein kinase B (AKT)-related signaling, thereby supporting malignant progression.[29] Because activation of the phosphoinositide 3-kinase-AKT pathway is known to foster an immunosuppressive tumor environment[30], *RAC3* overexpression may indirectly contribute to impaired antitumor immunity. *ZNF703* is frequently upregulated in solid tumors and promotes epithelial-to-mesenchymal transition (EMT), a process known to facilitate invasion and to attenuate immune detection, thereby linking *ZNF703* to both aggressive disease and potential immune evasion.[31,32] *DLL3* encodes an atypical Notch ligand aberrantly expressed in neuroendocrine malignancies, altering tumor cell communication, and has emerged as an actionable immune target in antibody drug conjugate and T-cell redirecting therapies.[33] Finally, *GSTP1* encodes a detoxification enzyme, which contributes to resistance against platinum-based chemotherapy and is associated with unfavorable outcomes across several cancer types.[34] These findings suggest that the transcriptional programs activated in the high-risk group favor tumor progression and dampen antitumor immunity.

Given the known crosstalk between immune cells and tumor-intrinsic signaling,[35] we performed functional enrichment analysis to contextualize our gene-level observations in melanoma. The DEGs were significantly enriched in immune-related processes, including leukocyte-mediated immunity, T-cell activation, and leukocyte proliferation (Figure 2C). These results suggest that enhanced immune activity is a key feature of the low-risk group, which may explain their improved survival.

To gain a deeper insight into the immune contexture, we applied CIBERSORT to deconvolve the bulk

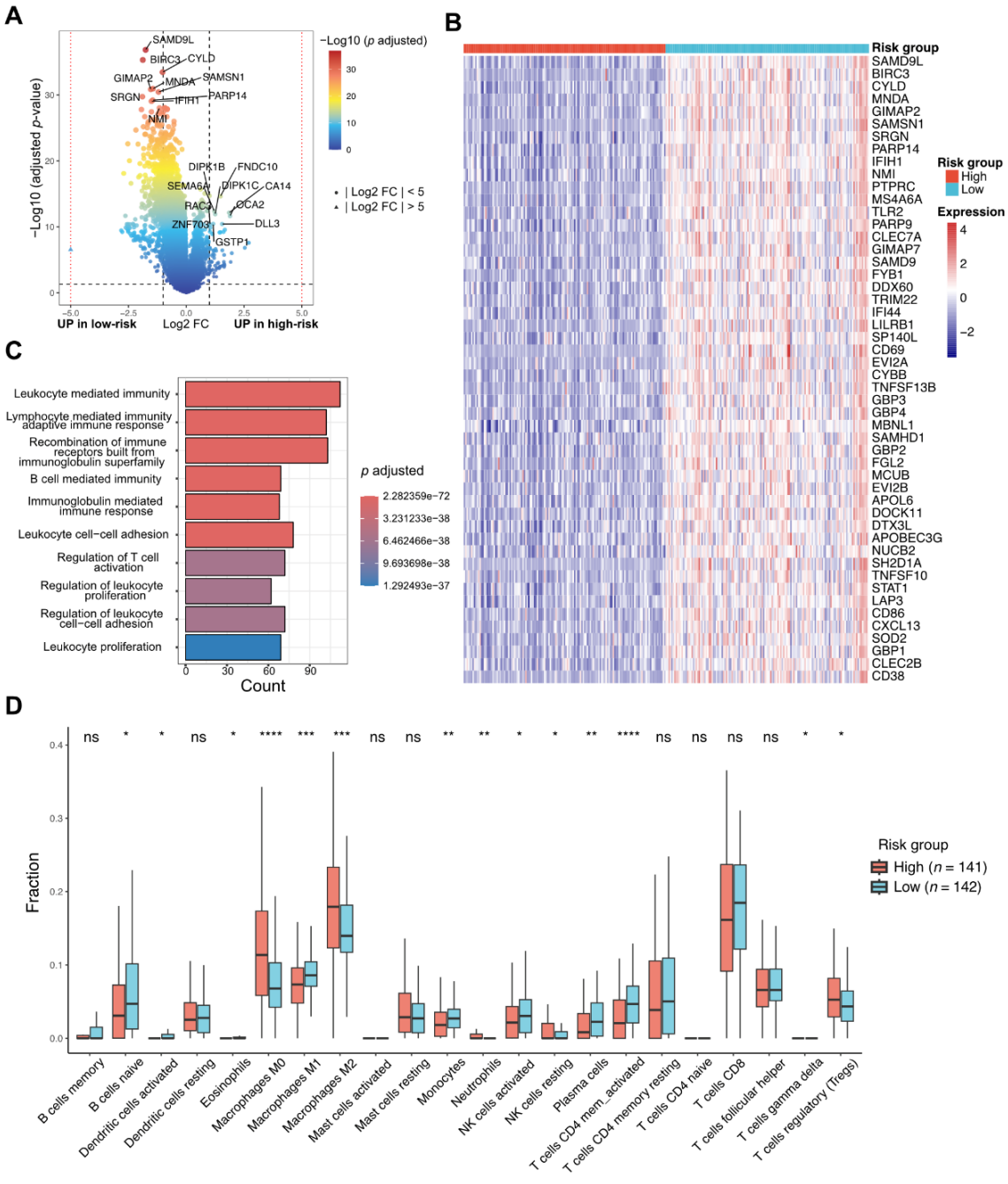


Figure 2. Differential expression and immune infiltration patterns associated with the autophagy-related prognostic signature. (A) Volcano plot showing DEGs between two risk groups in the training set. (B) Heatmap of the top 50 DEGs demonstrating distinct clustering of patients by risk status. (C) Bar plot of GO biological process terms significantly upregulated for the DEGs. The bar length represents the number of upregulated genes (count). The color intensity of bars corresponds to the statistical significance (FDR-corrected *p*-value). (D) Bar plot demonstrating differential abundance of 22 immune cell subsets between risk groups, as estimated by CIBERSORT. Statistical significance was determined by the Wilcoxon rank-sum test in D.
Notes: *$p < 0.05$; **$p < 0.01$; ***$p < 0.001$; ****$p < 0.0001$.
Abbreviations: DEGs: Differentially expressed genes; FC: Fold change; GO: Gene ontology; ns, not significant.

transcriptomic data into relative proportions of 22 immune cell subsets, as described in Section 2 (Materials and Methods). Substantial differences in immune infiltration were observed between the two groups (Figure 2D). The high-risk group exhibited elevated proportions of M2 macrophages and regulatory T cells (Tregs), both of which are known to dampen antitumor immunity and promote immune evasion.[36,37] Tregs suppress cytotoxic T-cell activity and weaken immune surveillance, while M2 macrophages also facilitate tumor growth and angiogenesis by releasing cytokines.[38–40] The low-risk group, on the other hand, showed greater infiltration of naïve B cells, plasma cells, activated natural killer (NK) cells, and both cluster of differentiation (CD)4$^+$ memory and CD8$^+$ cytotoxic T lymphocytes, consistent with an immune-inflamed tumor microenvironment. Similar findings from previous studies have linked strong infiltration of helper and cytotoxic immune cells with better survival in melanoma.[41]

Taken together, these results suggest that the autophagy-related prognostic signature not only stratifies patients by survival outcomes but also captures distinct immune landscapes. The low-risk group is characterized by protective immune programs and enhanced antitumor surveillance, whereas the high-risk group is dominated by oncogenic drivers and features an immunosuppressive microenvironment.

3.3. Validation of the immune landscape in test and external cohorts

We next validated the immune patterns in the independent TCGA test cohort by examining immune-related transcriptional programs and infiltration profiles. Consistent with the training set, the low-risk group showed markedly elevated immune pathway activity (Figure 3A) that collectively orchestrates effective tumor immune surveillance.[42,43] For instance, the regulation of T-cell activation directly influences cytotoxic T-lymphocyte expansion and effector function, processes that have been repeatedly linked to durable responses in melanoma patients treated with immunotherapies.[41] Likewise, B-cell-driven immune activity and plasma cell maturation promote antibody secretion and aid in antigen presentation and T-cell activation, potentiating antitumor immune responses.[44] The enrichment of these immune-activating programs in the low-risk group therefore provides a mechanistic rationale for their superior survival outcomes. To further assess generalizability, we validated these findings in an independent external cohort (GSE65904). The low-risk group displayed a similar enrichment of immune-related pathways (Figure 3B), suggesting that the immune activation associated with the autophagy-related risk score is reproducible across datasets.

Building on these pathway-level findings, we sought to determine if the transcriptional differences translated into a distinct cellular landscape within the tumor microenvironment. Applying CIBERSORT to deconvolute the immune cell composition, we identified consistent and reproducible shifts across both the TCGA test set and the external GSE65904 cohort. High-risk tumors contained a higher proportion of immunosuppressive cell populations, particularly M2 macrophages and regulatory T cells, whereas low-risk ones were characterized by elevated plasma cells, activated NK cells, CD4$^+$ memory T lymphocytes, and CD8$^+$ T lymphocytes (Figures 3C–3D). These infiltration patterns closely mirrored the immune landscapes in the training set, suggesting that the autophagy-based risk score robustly captures melanoma immune polarization across independent datasets.

Taken together, our analysis goes beyond simple prognosis prediction by linking the autophagy-related-gene signature to an immune-activated tumor microenvironment. The consistency of these immune-related patterns across the training, test, and external validation cohorts further indicates that the constructed signature captures key immune features that are conserved in melanoma. This highlights the potential biological significance of the immune landscape in shaping the tumor's behavior, which may contribute to the prognostic relevance of the signature.

3.4. Correlation between immune checkpoint expression and immune cell infiltration

To further delineate the immune context of the autophagy-related prognostic signature, we examined the expression patterns of canonical immune checkpoint molecules in the TCGA training set. The five canonical inhibitory checkpoints (*PDCD1*, *CD274*, *CTLA4*, *LAG3*, and *TIGIT*) were significantly upregulated in the low-risk group compared to the high-risk one (Figure 4A). Inhibitory molecules, such as programmed cell death protein 1 (PD-1) (encoded by *PDCD1*) and programmed death-ligand 1 (PD-L1) (encoded by *CD274*), often act as a brake to prevent T-cell overactivation.[45] Although tumor cells exploit their interactions with CD8$^+$ T lymphocytes to evade immune surveillance, their expression is a reliable indicator of pre-existing antitumor immunity.[46] *PDCD1* expression often correlates with infiltration of effector T cells and favorable outcomes in melanoma patients undergoing checkpoint blockade therapy.[47] Similarly, *CD274* expression has been associated with higher response rates to anti-PD-1/PD-L1 therapy and is frequently observed in tumors exhibiting an immune-inflamed phenotype.[48] Cytotoxic T-lymphocyte-associated protein 4 (CTLA-4) is a well-established coinhibitory receptor, and combination PD-1/CTLA-4

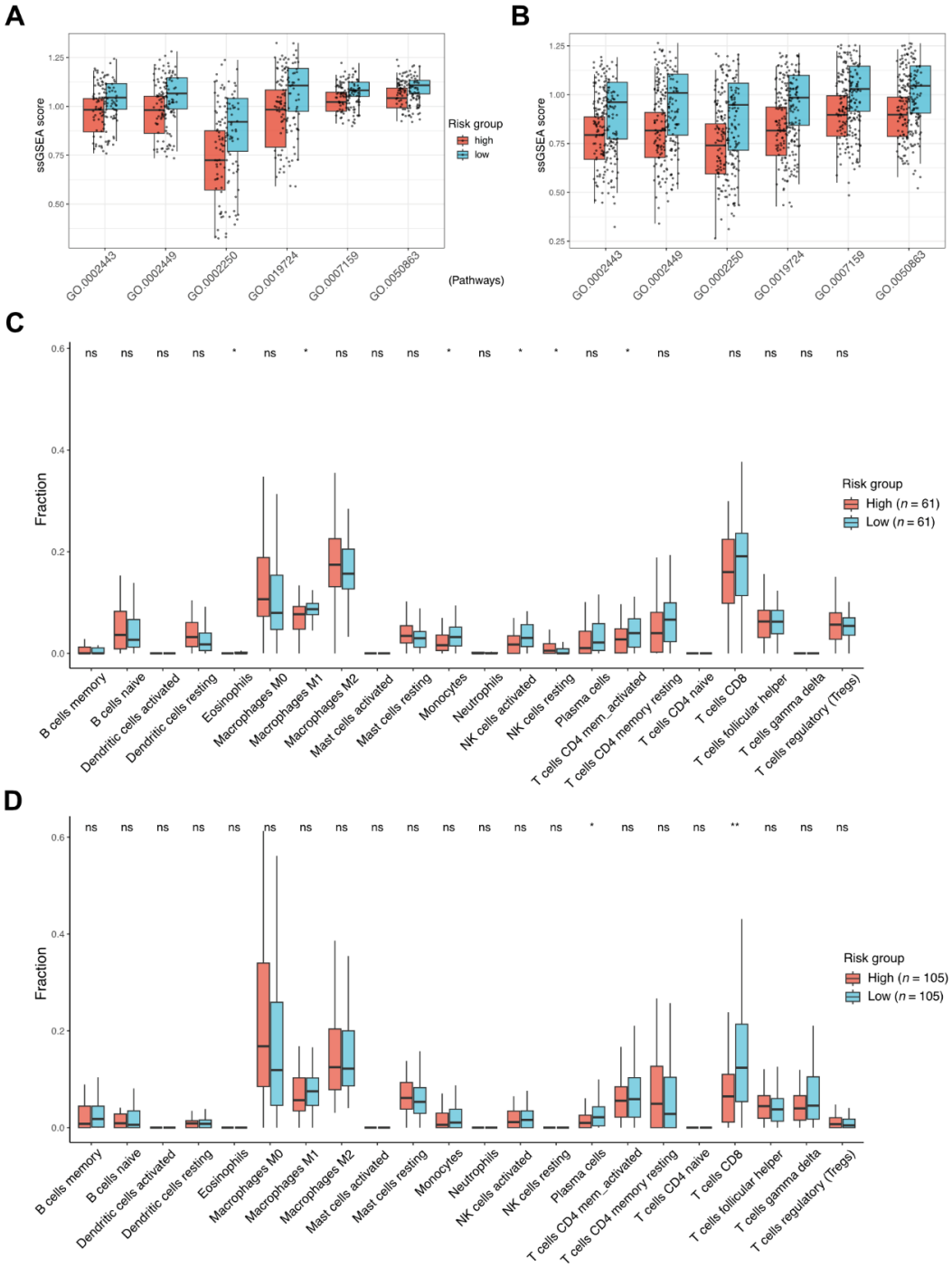


Figure 3. Immune-related pathways and immune infiltration patterns stratified by the autophagy-related prognostic signature. (A–B) Boxplots showing single-sample gene set enrichment analysis enrichment scores of immune-related pathways in the TCGA test set (A) and the external validation dataset GSE65904 (B). Pathways include leukocyte-mediated immunity (GO:0002443, GO:0002449), adaptive immune response (GO:0002250), B cell-mediated immunity (GO:0019724), leukocyte cell–cell adhesion (GO:0007159), and regulation of T-cell activation (GO:0050863). (C–D) Boxplots showing the relative abundance of 22 immune cell types estimated by CIBERSORT in the TCGA test set (C) and the GSE65904 validation cohort (D). Statistical significance was determined by the Wilcoxon rank-sum test in D.

Notes: $^{*}p < 0.05$; $^{**}p < 0.01$.

Abbreviations: GO: Gene ontology; NK: Natural killer; ns, not significant; ssGSEA: Single-sample gene set enrichment analysis; TCGA: The Cancer Genome Atlas.

inhibition (for example, nivolumab plus ipilimumab) has been established for first-line treatment of metastatic melanoma.[49] In addition, lymphocyte-activation gene 3 (LAG-3) and T-cell immunoreceptor with immunoglobulin and immunoreceptor tyrosine-based inhibitory motif domains (TIGIT) have emerged more recently as promising checkpoint targets: for instance, the RELATIVITY-047 trial demonstrated a significant improvement in progression-free survival with combined LAG-3 and PD-1 blockade compared to PD-1 monotherapy.[50,51] The coordinated expression of 7these checkpoints, which are central regulators of T-cell activation and immune homeostasis[52], often reflects an immune-inflamed tumor phenotype, as strongly evidenced by recent investigations.[53] Moreover, studies indicate that within the melanoma tumor niche, $CD8^+$ T lymphocytes exhibiting a dysfunctional phenotype often co-express TIGIT[54], further linking checkpoint upregulation with effector T-cell infiltration and immune activation in melanoma.

To determine whether checkpoint expression was associated with immune infiltration, we conducted Spearman correlation tests to evaluate associations between immune checkpoint expression level and immune cell composition inferred by CIBERSORT analysis. As shown in Figure 4B, checkpoint expression correlated positively with $CD8^+$ T lymphocytes and activated NK cells. This suggests that in the low-risk group, increased checkpoint expression reflects an ongoing antitumor immune response, driven by effector cell infiltration, rather than indicating intrinsic immune suppression, which aligns with recent studies.[55]

These findings suggest that low-risk tumors exhibit an immune-active microenvironment, with traits commonly associated with an "immune-hot" tumor microenvironment, a term used to describe tumors with high expression of immune checkpoints, abundant effector T lymphocytes and NK-cell infiltration, and elevated interferon signaling.[50,56] Such "immune-

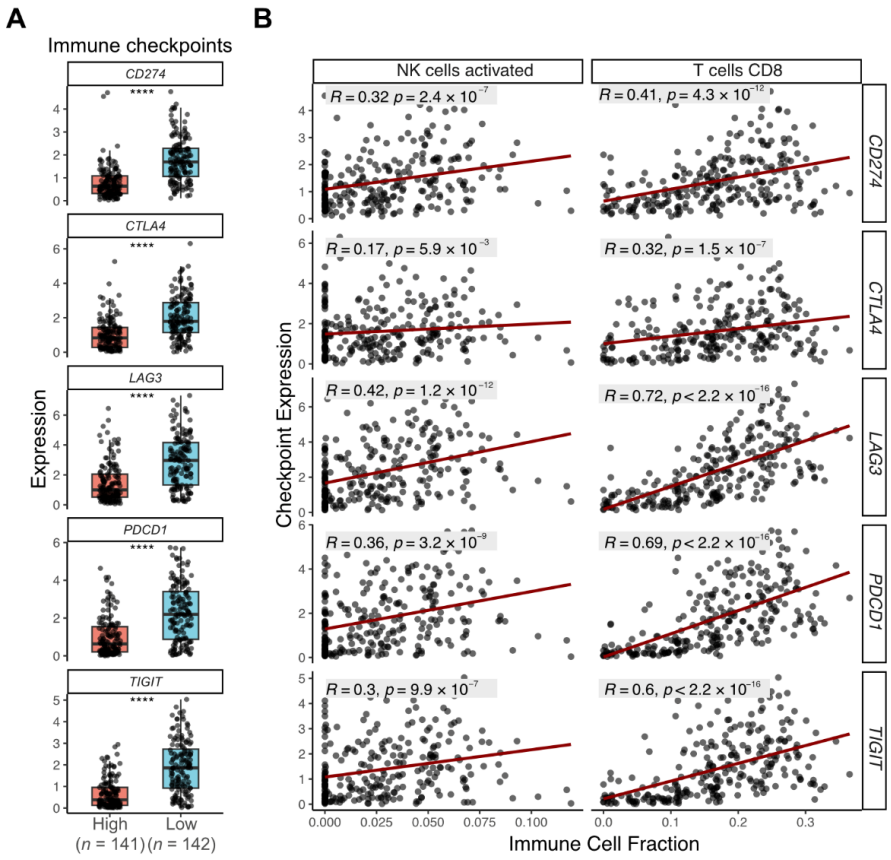


Figure 4. Immune checkpoint expression and correlation with immune infiltration. (A) Boxplot showing the expression of five canonical immune checkpoint genes (*PDCD1*, *CD274*, *CTLA4*, *LAG3*, *TIGIT*) between high- and low-risk groups in The Cancer Genome Atlas training set. (B) Scatter plots showing Spearman correlations between checkpoint gene expression and the fractions of cluster of differentiation $(CD)8^+$ T cells and activated natural killer (NK) cells estimated by CIBERSORT.

hot" tumors generally have favorable prognoses and increased sensitivities to immune checkpoint inhibitors.[57] Given these immune-inflamed characteristics, we next investigated whether the autophagy-related-gene signature we constructed could distinguish responses to therapy in melanoma patients undergoing immune checkpoint blockade.

3.5. Independent validation of the autophagy-related-gene signature in an anti-programmed cell death protein 1-treated melanoma cohort

To further assess the potential clinical relevance of our autophagy-related prognostic signature in the context of immunotherapy, we performed an independent validation using the publicly available dataset GSE91061, which includes melanoma patients treated with anti-PD-1 therapy.[42] Risk scores showed an increasing trend from responders to stable disease, then to non-responders, although the trend was not statistically significant (Figure A2A), likely due to the limited sample size and heterogeneous clinical and sequencing conditions. Consistent with findings from the TCGA training set, tumors in the low-risk group exhibited significantly higher expression of key immune checkpoint genes (Figure A2B).

Together, these observations suggest that the autophagy-related-gene signature is associated with differences in immune activity within the tumor microenvironment, although its predictive value for immunotherapy response remains to be validated in larger, well-annotated clinical cohorts.

4. Discussion

In this study, we developed and validated a comprehensive 102-autophagy-related-gene prognostic signature that robustly stratifies melanoma patients into distinct risk groups across multiple independent cohorts (Figure 5). Compared with prior autophagy-based models that

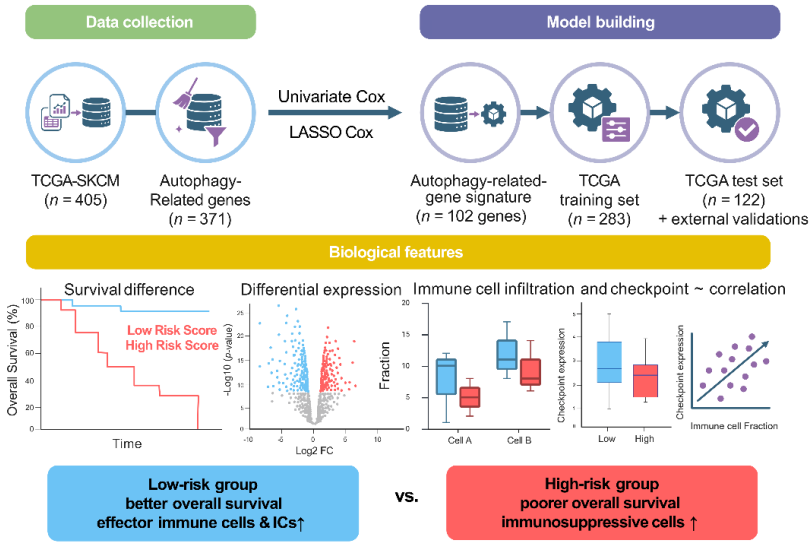


Figure 5. Overview of study workflow and main findings. The overall analytical workflow of the study is illustrated. Transcriptomic and clinical data of melanoma (TCGA-SKCM, n = 405) were collected, and 371 autophagy-related genes were selected. Univariate and LASSO Cox regression analyses were applied to build an autophagy-related-gene signature (n = 102 genes). The patients from the TCGA cohort were randomly assigned to a training set (n = 283) or a test set (n = 122), followed by validation in external melanoma datasets. The model effectively discriminated between two risk groups (high vs. low) that exhibited significantly different overall survival. Differential expression and immune deconvolution analyses revealed that the low-risk group exhibited elevated infiltration of immune cells and increased expression of immune checkpoints, indicating an immune-inflamed tumor microenvironment, whereas high-risk tumors were enriched in immunosuppressive cell subsets.
Abbreviations: FC: Fold change; LASSO: Least Absolute Shrinkage and Selection Operator; SKCM: Skin cutaneous melanoma; TCGA: The Cancer Genome Atlas.

primarily focused on prognostic classification[14–16], this work provides an integrative view linking autophagy-related transcriptional programs with the immune landscape of melanoma. By integrating transcriptomic, pathway, and immune-cell composition analyses, this study provides a comprehensive view of how autophagy correlates with tumor-immune states, thereby offering insights into the biological basis of risk stratification and potential implications for immunotherapy research.

Critically, the tumor immune landscape differed significantly between risk groups. In low-risk tumors, we observed higher expression of several immune-regulatory genes (including *SAMD9L*, *BIRC3*, *CYLD*, *IFIH1*) that are functionally linked to innate and adaptive antiviral/antitumor signaling. Conversely, genes upregulated in the high-risk group (e.g., *RAC3*, *ZNF703*, *DLL3*, *GSTP1*) have been implicated in oncogenic signaling, EMT, and pro-tumor programs that may promote immune evasion, consistent with the broader programs previously associated with poor response to checkpoint blockade in melanoma.[58,59]

Functional enrichment analysis demonstrated that genes upregulated in the low-risk group were involved in immune-related pathways. This is consistent with earlier work showing that active T-cell and B-cell programs strongly predict a favorable prognosis and are often associated with responsiveness to immune checkpoint inhibitors.[58,60] The convergence of gene-level and pathway-level evidence suggests that the autophagy-related-gene signature captures an immune-active tumor state rather than merely reflecting general transcriptional variation. Moreover, analysis of immune cell composition showed that the low-risk group had greater infiltration of effector cells, such as $CD8^+$ cytotoxic T lymphocytes and activated NK cells. This pattern suggests an inflamed and immune-active tumor environment. In contrast, the high-risk group showed higher levels of M2 macrophages and regulatory T cells, indicating an immunosuppressive setting often associated with therapeutic resistance.[61,62] These opposing immune states, often described as "immune-inflamed" versus "immune-suppressed" phenotypes, are in line with established immuno-oncologic paradigms[63–65] and suggest that autophagy-related gene expression may serve as a transcriptional correlate of immune polarization in melanoma. To better understand this pattern, we examined the expression of five canonical immune checkpoint genes, all of which were significantly upregulated in the low-risk group. Although these molecules mediate immune inhibition, their upregulation usually reflects an adaptive reaction to sustained immune activation, rather than indicating intrinsic immune suppression.[66] In numerous studies, checkpoint expression often marks tumors with effector T-lymphocyte infiltration and interferon signaling, representing an adaptive brake on excessive immune activity.[67,68] This explanation is supported by the positive relationship between checkpoint expression and the abundance of $CD8^+$ T cells and activated NK cells. Therefore, the higher checkpoint expression observed in low-risk tumors may reflect a dynamic equilibrium between immune activation and regulation, as seen in tumors with a favorable prognosis and greater response to immunotherapy.[69,70]

To explore the possible clinical meaning of this immune-related pattern, we performed an exploratory validation using an anti-PD-1-treated melanoma dataset (GSE91061).[42] The results showed that patients who did not respond to therapy tended to have higher risk scores, although the difference was not statistically significant. Tumors in the low-risk group showed higher expression of key immune checkpoint genes, consistent with the immune-active gene expression pattern seen in the TCGA cohort. These results indicate that the autophagy-based signature reflects two distinct immune states, one immune-active and the other immune-suppressed. The findings also suggest that this signature may help describe the interaction between tumor cells and the immune system. However, further validation in larger and well-characterized clinical cohorts is needed to confirm its predictive value for immune checkpoint therapy.

The relationship between autophagy and antitumor immunity is complex and varies depending on the cellular and microenvironmental context. In immune-activated environments, autophagy can support antigen presentation and promote effector cell activation. These effects strengthen immune surveillance and contribute to tumor control.[71,72] In contrast, within tumor cells, autophagy may act as a protective mechanism that weakens immune recognition. For example, by degrading major histocompatibility complex class I molecules, tumor cells can reduce antigen visibility to cytotoxic T lymphocytes.[73] Autophagy has also been shown to sustain tumor growth and immune evasion by activating pro-survival pathways, such as signal transducer and activator of transcription 3 signaling, and by clearing cytotoxic granules released by NK cells.[74,75] The coexistence of these opposite functions may underlie the dual prognostic associations of autophagy across cancers, underscoring the need for cell-type-specific and spatially resolved investigations in melanoma.

Several limitations of this study should be acknowledged. First, our analyses were based on bulk RNA-seq data, which cannot fully capture the spatial distribution or heterogeneity of immune cells within the

tumor microenvironment. Second, although the 102-gene signature demonstrated robust performance across multiple independent datasets, the study design remains retrospective, and prospective validation in patients undergoing immunotherapy will be necessary to confirm its predictive value. Third, factors such as tumor mutational burden and neoantigen load, which are known to influence immune responses[76], were not incorporated, and they could further refine prognostic accuracy. Fourth, while our analyses suggest biological associations between autophagy and immune activation, experimental studies are needed to establish causal mechanisms. Finally, we acknowledge that the 102-gene signature is relatively large, which may limit its direct clinical applicability. Nevertheless, the comprehensive transcriptomic information captured by the full model substantially enhances prognostic performance. Future efforts will aim to balance clinical feasibility and model complexity by refining the signature, integrating biological relevance and interpretability to develop a smaller, clinically practical gene panel.

In conclusion, this study identifies an autophagy-related-gene signature that independently predicts melanoma prognosis and reflects differences in immune activity within the tumor microenvironment. While its relationship with immunotherapy response remains exploratory, the signature suggests a biological link between autophagy and immune polarization. These insights may provide a foundation for future research combining autophagy modulation with immune-based cancer therapies.

5. Conclusion

In summary, we constructed a prognostic model based on an autophagy-related-gene signature that effectively distinguishes melanoma patients with different survival outcomes. Tumors classified as low-risk exhibited an active immune contexture with increased infiltration of effector immune cells. In contrast, high-risk tumors were marked by oncogenic signaling pathways and an immunosuppressive milieu. These findings suggest a close link between autophagy-related transcriptional programs and immune regulation in melanoma. Although additional studies are needed to determine its utility in predicting responses to immunotherapy, our work highlights the value of integrating autophagy markers into melanoma prognosis and provides a framework for future translational research in this area.

Acknowledgments

None.

Funding

This study is jointly supported by Natural Science Foundation of the New Era Longjiang Outstanding Master's and Doctoral Dissertation Funding Program (Grant No.LJYXL2022-074), The Scientific Research and Innovation Foundation of The First Affiliated Hospital of Harbin Medical University (Grant No.2023M30), National Key R&D Programmes (NKPs) of China (Grant No. 2022YFC3601800), and General project of Chongqing Joint Fund of Science and Technology (Grant No. CSTB2024NSCQ-LMX0016).

Conflict of interest

Mingzhu Yin is the Editor-in-Chief of this journal, but was not in any way involved in the editorial and peer-review process conducted for this paper, directly or indirectly. Separately, other authors declared that they have no known competing financial interests or personal relationships that could have influenced the work reported in this paper.

Author contributions

Conceptualization: Xiyuan Zhang, Mingzhu Yin
Formal analysis: Yadong Xue, Xiyuan Zhang
Investigation: Yadong Xue, Xiyuan Zhang
Methodology: Xiyuan Zhang, Yunjin Xie
Writing–original draft: Yadong Xue, Xiyuan Zhang
Writing–review & editing: All authors

Ethics approval and consent to participate

Not applicable.

Consent for publication

Not applicable.

Availability of data

The RNA-seq data and matched clinical information, including gender, age, tumor stage, T/N/M stage, overall survival (OS), and OS time for TCGA-SKCM patients, were obtained from the University of California, Santa Cruz Xena database (https://xenabrowser.net/datapages/). Raw expression profiles and survival data for the external validation cohorts GSE215119, GSE190113, GSE65904, and GSE91061 were downloaded from the Gene Expression Omnibus (https://www.ncbi.nlm.nih.gov/geo/). The autophagy-related genes were curated from the Human Autophagy Database (http://www.autophagy.lu/) for subsequent analysis.

References

1. Arnold M, Singh D, Laversanne M, *et al.* Global Burden of Cutaneous Melanoma in 2020 and Projections to 2040. *JAMA Dermatol.* 2022;158(5):495-503.

doi: 10.1001/jamadermatol.2022.0160

2. Sigalotti L, Covre A, Fratta E, *et al.* Epigenetics of human cutaneous melanoma: setting the stage for new therapeutic strategies. *J Transl Med*. 2010;8:56.

doi: 10.1186/1479-5876-8-56

3. Karimkhani C, Green AC, Nijsten T, *et al.* The global burden of melanoma: results from the Global Burden of Disease Study 2015. *Br J Dermatol*. 2017;177(1):134-140.

doi: 10.1111/bjd.15510

4. Centeno PP, Pavet V, Marais R. The journey from melanocytes to melanoma. *Nat Rev Cancer*. 2023;23(6):372-390.

doi: 10.1038/s41568-023-00565-7

5. Eddy K, Chen S. Overcoming Immune Evasion in Melanoma. *Int J Mol Sci*. 2020;21(23):8984.

doi: 10.3390/ijms21238984

6. Liguoro D, Fattore L, Mancini R, Ciliberto G. Drug tolerance to target therapy in melanoma revealed at single cell level: What next? *Biochim Biophys Acta Rev Cancer*. 2020;1874(2):188440.

doi: 10.1016/j.bbcan.2020.188440

7. Robertson BM, Fane ME, Weeraratna AT, Rebecca VW. Determinants of resistance and response to melanoma therapy. *Nat Cancer*. 2024;5(7):964-982.

doi: 10.1038/s43018-024-00794-1

8. Ascierto PA, Bifulco C, Galon J, *et al.* The Great Debate at "Immunotherapy Bridge", Naples, December 5, 2019. *J Immunother Cancer*. 2020;8(2):e000921.

doi: 10.1136/jitc-2020-000921

9. Bortnik S, Gorski SM. Clinical Applications of Autophagy Proteins in Cancer: From Potential Targets to Biomarkers. *Int J Mol Sci*. 2017;18(7):1496.

doi: 10.3390/ijms18071496

10. Gülow K, Tümen D, Kunst C. The Important Role of Protein Kinases in the p53 Sestrin Signaling Pathway. *Cancers*. 2023;15(22):5390.

doi: 10.3390/cancers15225390

11. Yu YS, Kim IS, Baek SH. Decoding the dual role of autophagy in cancer through transcriptional and epigenetic regulation. *FEBS Lett*. 2025;599(16):2237-2249.

doi: 10.1002/1873-3468.70060

12. Vona R, Cittadini C, Ortona E, Matarrese P. Sex Disparity in Cancer: Role of Autophagy and Estrogen Receptors. *Cells*. 2025;14(4):273.

doi: 10.3390/cells14040273

13. Ndoye A, Weeraratna AT. Autophagy- An emerging target for melanoma therapy. *F1000Research*. 2016;5:1888.

doi: 10.12688/f1000research.8347.1

14. Wan Q, Jin L, Su Y, Liu Y, Li C, Wang Z. Development and validation of autophagy-related-gene biomarker and nomogram for predicting the survival of cutaneous melanoma. *IUBMB Life*. 2020;72(7):1364-1378.

doi: 10.1002/iub.2258

15. Fei H, Chen X. Establishment and validation of an autophagy-related prognostic signature for survival predicting in cutaneous melanoma. *Am J Cancer Res*. 2021;11(12):5979-5991.

16. Liao S, He J, Liu C, *et al.* Construction of autophagy prognostic signature and analysis of prospective molecular mechanisms in skin cutaneous melanoma patients. *Medicine*. 2021;100(22):e26219.

doi: 10.1097/MD.0000000000026219

17. Zhang L, Zhu Y, Zhang J, Zhang L, Chen L. Inhibiting Cytoprotective Autophagy in Cancer Therapy: An Update on Pharmacological Small-Molecule Compounds. *Front Pharmacol*. 2022;13:966012.

doi: 10.3389/fphar.2022.966012

18. Tan Y, Zhu J, Hashimoto K. Autophagy-related gene model as a novel risk factor for schizophrenia. *Transl Psychiatry*. 2024;14(1):94.

doi: 10.1038/s41398-024-02767-5

19. Newman AM, Liu CL, Green MR, *et al.* Robust enumeration of cell subsets from tissue expression profiles. *Nat Methods*. 2015;12(5):453-457.

doi: 10.1038/nmeth.3337

20. Feng Y, Liu L, Xie Y, Yin M. Development of a novel risk model for stratifying skin cutaneous melanoma patients based on prognostic senescence-related genes. *Eurasian J Med Oncol*. 2025;0(0):8574.

doi: 10.36922/ejmo.8574

21. Balch CM, Gershenwald JE, Soong S jaw, *et al.* Final version of 2009 AJCC melanoma staging and classification. *J Clin Oncol.* 2009;27(36):6199-6206.

doi: 10.1200/JCO.2009.23.4799

22. Peng S, Meng X, Zhang F, *et al.* Structure and function of an effector domain in antiviral factors and tumor suppressors SAMD9 and SAMD9L. *Proc Natl Acad Sci*. 2022;119(4):e2116550119.

doi: 10.1073/pnas.2116550119

23. Wong JC, Bryant V, Lamprecht T, *et al.* Germline SAMD9 and SAMD9L mutations are associated with extensive genetic evolution and diverse hematologic outcomes. *JCI Insight*. 2018;3(14):e121086.

doi: 10.1172/jci.insight.121086

24. Frazzi R. BIRC3 and BIRC5: multi-faceted inhibitors in cancer. *Cell Biosci*. 2021;11(1):8.

doi: 10.1186/s13578-020-00521-0

25. Massoumi R, Chmielarska K, Hennecke K, Pfeifer A, Fässler R. Cyld inhibits tumor cell proliferation by blocking Bcl-3-dependent NF-kappaB signaling. *Cell*. 2006;125(4):665-677.

doi: 10.1016/j.cell.2006.03.041

26. Cui Z, Kang H, Grandis JR, Johnson DE. CYLD Alterations in the Tumorigenesis and Progression of Human Papillomavirus-Associated Head and Neck Cancers. *Mol Cancer Res*. 2021;19(1):14-24.

doi: 10.1158/1541-7786.MCR-20-0565

27. Zhu G, Herlyn M, Yang X. TRIM15 and CYLD regulate ERK activation via lysine-63-linked polyubiquitination. *Nat Cell Biol*. 2021;23(9):978-991.

doi: 10.1038/s41556-021-00732-8

28. Dhir A, Dhir S, Borowski LS, *et al.* Mitochondrial double-stranded RNA triggers antiviral signalling in humans. *Nature*. 2018;560(7717):238-242.

doi: 10.1038/s41586-018-0363-0

29. Fernández Larrosa PN, Ruíz Grecco M, Mengual Gómez D, *et al.* RAC3 more than a nuclear receptor coactivator: a key inhibitor of senescence that is downregulated in aging. *Cell Death Dis*. 2015;6(10):e1902.

doi: 10.1038/cddis.2015.218

30. Collins NB, Al Abosy R, Miller BC, *et al.* PI3K activation allows immune evasion by promoting an inhibitory myeloid tumor microenvironment. *J Immunother Cancer*. 2022;10(3):e003402.

doi: 10.1136/jitc-2021-003402

31. Pastushenko I, Blanpain C. EMT Transition States during Tumor Progression and Metastasis. *Trends Cell Biol*. 2019;29(3):212-226.

doi: 10.1016/j.tcb.2018.12.001

32. Wang H, Xu H, Ma F, *et al.* Zinc finger protein 703 induces EMT and sorafenib resistance in hepatocellular carcinoma by transactivating CLDN4 expression. *Cell Death Dis*. 2020;11(4):225.

doi: 10.1038/s41419-020-2422-3

33. Rudin CM, Reck M, Johnson ML, *et al.* Emerging therapies targeting the delta-like ligand 3 (DLL3) in small cell lung cancer. *J Hematol OncolJ Hematol Oncol*. 2023;16(1):66.

doi: 10.1186/s13045-023-01464-y

34. Sawers L, Ferguson MJ, Ihrig BR, *et al.* Glutathione S-transferase P1 (GSTP1) directly influences platinum drug chemosensitivity in ovarian tumour cell lines. *Br J Cancer*. 2014;111(6):1150-1158.

doi: 10.1038/bjc.2014.386

35. Wojdasiewicz P, Poniatowski ŁA, Kotela A, *et al.* Comparative Analysis of the Occurrence and Role of CX3CL1 (Fractalkine) and Its Receptor CX3CR1 in Hemophilic Arthropathy and Osteoarthritis. *J Immunol Res*. 2020;2020:2932696.

doi: 10.1155/2020/2932696

36. Chen S, Saeed AFUH, Liu Q, *et al.* Macrophages in immunoregulation and therapeutics. *Signal Transduct Target Ther*. 2023;8(1):207.

doi: 10.1038/s41392-023-01452-1

37. Zhou Z, Xu J, Liu S, *et al.* Infiltrating treg reprogramming in the tumor immune microenvironment and its optimization for immunotherapy. *Biomark Res*. 2024;12(1):97.

doi: 10.1186/s40364-024-00630-9

38. Wang S, Wang J, Chen Z, *et al.* Targeting M2-like tumor-associated macrophages is a potential therapeutic approach to overcome antitumor drug resistance. *npj Precis Oncol*. 2024;8(1):31.

doi: 10.1038/s41698-024-00522-z

39. Monjaras-Avila CU, Lorenzo-Leal AC, Luque-Badillo AC, D'Costa N, Chavez-Muñoz C, Bach H. The Tumor Immune Microenvironment in Clear Cell Renal Cell Carcinoma. *Int J Mol Sci*. 2023;24(9):7946.

doi: 10.3390/ijms24097946

40. Zhou Z, Zhang X, Zhu S, *et al.* Crizotinib: A Novel Strategy to Reverse Immunosuppression in Melanoma by Targeting Lactate Transport. *MedComm*. 2025;6(8):e70286.

doi: 10.1002/mco2.70286

41. Salmon H, Remark R, Gnjatic S, Merad M. Host tissue determinants of tumour immunity. *Nat Rev Cancer*. 2019;19(4):215-227.

doi: 10.1038/s41568-019-0125-9

42. Riaz N, Havel JJ, Makarov V, *et al.* Tumor and Microenvironment Evolution during Immunotherapy with Nivolumab. *Cell*. 2017;171(4):934-949.e16.

doi: 10.1016/j.cell.2017.09.028

43. Wang Z, Lu Z, Lin S, *et al.* Leucine-tRNA-synthase-2-expressing B cells contribute to colorectal cancer immunoevasion. *Immunity*. 2022;55(6):1067-1081.e8.

doi: 10.1016/j.immuni.2022.04.017

44. Helmink BA, Reddy SM, Gao J, *et al.* B cells and tertiary lymphoid structures promote immunotherapy response. *Nature*. 2020;577(7791):549-555.

doi: 10.1038/s41586-019-1922-8

45. Lv M, Chen M, Zhang R, *et al.* Manganese is critical for antitumor immune responses via cGAS-STING and improves the efficacy of clinical immunotherapy. *Cell Res*. 2020;30(11):966-979.

doi: 10.1038/s41422-020-00395-4

46. Hao D, Wang G, Yang W, *et al.* Reactive versus Constitutive:

Reconcile the Controversial Results about the Prognostic Value of PD-L1 Expression in cancer. *Int J Biol Sci*. 2019;15(9):1933-1941.

doi: 10.7150/ijbs.33297

47. Monti M, Consoli F, Vescovi R, Bugatti M, Vermi W. Human Plasmacytoid Dendritic Cells and Cutaneous Melanoma. *Cells*. 2020;9(2):417.

doi: 10.3390/cells9020417

48. Tu J, Xu H, Ma L, *et al.* Nintedanib enhances the efficacy of PD-L1 blockade by upregulating MHC-I and PD-L1 expression in tumor cells. *Theranostics*. 2022;12(2):747-766.

doi: 10.7150/thno.65828

49. Lu JE, Chang JR, Berry JL, In GK, Zhang-Nunes S. Clinical Update on Checkpoint Inhibitor Therapy for Conjunctival and Eyelid Melanoma. *Int Ophthalmol Clin*. 2020;60(2):77-89.

doi: 10.1097/IIO.0000000000000308

50. Wen J, Wang Y, Wang S, *et al.* Genetic and transcriptional insights into immune checkpoint blockade response and survival: lessons from melanoma and beyond. *J Transl Med*. 2025;23(1):467.

doi: 10.1186/s12967-025-06467-6

51. Su DG, Schoenfeld DA, Ibrahim W, *et al.* Digital spatial proteomic profiling reveals immune checkpoints as biomarkers in lymphoid aggregates and tumor microenvironment of desmoplastic melanoma. *J Immunother Cancer*. 2024;12(3):e008646.

doi: 10.1136/jitc-2023-008646

52. Yadav D, Puranik N, Meshram A, Chavda V, Lee PCW, Jin JO. How Advanced are Cancer Immuno-Nanotherapeutics? A Comprehensive Review of the Literature. *Int J Nanomed*. 2023;18:35-48.

doi: 10.2147/IJN.S388349

53. Zhao S, Zhao H, Yang W, Zhang L. The next generation of immunotherapies for lung cancers. *Nat Rev Clin Oncol*. 2025;22(8):592-616.

doi: 10.1038/s41571-025-01035-9

54. Hübbe ML, Jæhger DE, Andresen TL, Andersen MH. Leveraging Endogenous Dendritic Cells to Enhance the Therapeutic Efficacy of Adoptive T-Cell Therapy and Checkpoint Blockade. *Front Immunol*. 2020;11:578349.

doi: 10.3389/fimmu.2020.578349

55. Baessler A, Vignali DAA. T Cell Exhaustion. *Annu Rev Immunol*. 2024;42(1):179-206.

doi: 10.1146/annurev-immunol-090222-110914

56. Xiong L, Guo J, Lv J, Guo W, Qiu T. Radiotherapy-immunity lncRNA model predicts lung adenocarcinoma prognosis and treatment outcome and distinguishes between hot and cold tumors. *Discov Oncol*. 2025;16(1):455.

doi: 10.1007/s12672-025-02184-0

57. Shofolawe-Bakare OT, Stokes LD, Hossain M, Smith AE, Werfel TA. Immunostimulatory biomaterials to boost tumor immunogenicity. *Biomater Sci*. 2020;8(20):5516-5537.

doi: 10.1039/d0bm01183e

58. Hugo W, Zaretsky JM, Sun L, *et al.* Genomic and Transcriptomic Features of Response to Anti-PD-1 Therapy in Metastatic Melanoma. *Cell*. 2016;165(1):35-44.

doi: 10.1016/j.cell.2016.02.065

59. Gonzalez H, Hagerling C, Werb Z. Roles of the immune system in cancer: from tumor initiation to metastatic progression. *Genes Dev*. 2018;32(19-20):1267-1284.

doi: 10.1101/gad.314617.118

60. Yan J, Wu X, Yu J, Kong Y, Cang S. An Immune-Related Gene Pair Index Predicts Clinical Response and Survival Outcome of Immune Checkpoint Inhibitors in Melanoma. *Front Immunol*. 2022;13:839901.

doi: 10.3389/fimmu.2022.839901

61. Guo LJ, Wu J, Lu W, *et al.* Nanoparticles Modulating the Immune Microenvironment in Breast Cancer Treatment. *Int J Nanomed*. 2025;20:1367-1382.

doi: 10.2147/IJN.S492713

62. Donlon NE, Power R, Hayes C, Reynolds JV, Lysaght J. Radiotherapy, immunotherapy, and the tumour microenvironment: Turning an immunosuppressive milieu into a therapeutic opportunity. *Cancer Lett*. 2021;502:84-96.

doi: 10.1016/j.canlet.2020.12.045

63. Zhang S, Chen K, Liu H, *et al.* PMEL as a Prognostic Biomarker and Negatively Associated With Immune Infiltration in Skin Cutaneous Melanoma (SKCM). *J Immunother*. 2021;44(6):214-223.

doi: 10.1097/CJI.0000000000000374

64. Schaft N, Dörrie J, Schuler G, *et al.* The future of affordable cancer immunotherapy. *Front Immunol*. 2023;14:1248867.

doi: 10.3389/fimmu.2023.1248867

65. Adeshakin AO, Adeshakin FO, Yan D, Wan X. Regulating Histone Deacetylase Signaling Pathways of Myeloid-Derived Suppressor Cells Enhanced T Cell-Based Immunotherapy. *Front Immunol*. 2022;13:781660.

doi: 10.3389/fimmu.2022.781660

66. Krishnamurthy N, Nishizaki D, Lippman SM, *et al.* High CTLA-4 transcriptomic expression correlates with high expression of other checkpoints and with immunotherapy outcome. *Ther Adv Med Oncol*. 2024;16:17588359231220510.

doi: 10.1177/17588359231220510

67. Allen CT, Clavijo PE, Van Waes C, Chen Z. Anti-Tumor

Immunity in Head and Neck Cancer: Understanding the Evidence, How Tumors Escape and Immunotherapeutic Approaches. *Cancers*. 2015;7(4):2397-2414.

doi: 10.3390/cancers7040900

68. Liu C, Somasundaram A, Manne S, *et al.* Neuropilin-1 is a T cell memory checkpoint limiting long-term antitumor immunity. *Nat Immunol*. 2020;21(9):1010-1021.

doi: 10.1038/s41590-020-0733-2

69. Sun D, Liu J, Zhou H, *et al.* Classification of Tumor Immune Microenvironment According to Programmed Death-Ligand 1 Expression and Immune Infiltration Predicts Response to Immunotherapy Plus Chemotherapy in Advanced Patients With NSCLC. *J Thorac Oncol Off Publ Int Assoc Study Lung Cancer*. 2023;18(7):869-881.

doi: 10.1016/j.jtho.2023.03.012

70. Kockx MM, McCleland M, Koeppen H. Microenvironmental regulation of tumour immunity and response to immunotherapy. *J Pathol.* 2021;254(4):374-383.

doi: 10.1002/path.5681

71. Jeong J, Choi YJ, Lee HK. The Role of Autophagy in the Function of CD4+ T Cells and the Development of Chronic Inflammatory Diseases. *Front Pharmacol*. 2022;13:860146.

doi: 10.3389/fphar.2022.860146

72. Kang W, Hu J, Zhao Q, Song F. Identification of an Autophagy-Related Risk Signature Correlates With Immunophenotype and Predicts Immune Checkpoint Blockade Efficacy of Neuroblastoma. *Front Cell Dev Biol*. 2021;9:731380.

doi: 10.3389/fcell.2021.731380

73. Hashemi M, Mohandesi Khosroshahi E, Tanha M, *et al.* Targeting autophagy can synergize the efficacy of immune checkpoint inhibitors against therapeutic resistance: New promising strategy to reinvigorate cancer therapy. *Heliyon*. 2024;10(18):e37376.

doi: 10.1016/j.heliyon.2024.e37376

74. Li YY, Feun LG, Thongkum A, *et al.* Autophagic Mechanism in Anti-Cancer Immunity: Its Pros and Cons for Cancer Therapy. *Int J Mol Sci*. 2017;18(6):1297.

doi: 10.3390/ijms18061297

75. Schmid M, Fischer P, Engl M, Widder J, Kerschbaum-Gruber S, Slade D. The interplay between autophagy and cGAS-STING signaling and its implications for cancer. *Front Immunol*. 2024;15:1356369.

doi: 10.3389/fimmu.2024.1356369

76. Korpal M, Puyang X, Jeremy Wu Z, *et al.* Evasion of immunosurveillance by genomic alterations of PPARγ/RXRα in bladder cancer. *Nat Commun*. 2017;8(1):103.

doi: 10.1038/s41467-017-00147-w

Appendix

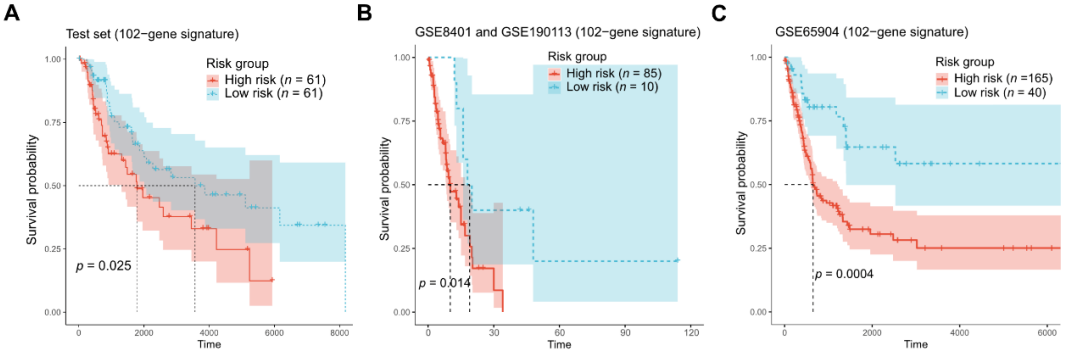


Figure A1. Validation of the prognostic signature in internal and external cohorts. (A) Kaplan–Meier curves showing overall survival differences between two risk groups in The Cancer Genome Atlas test set. (B–C) Validation of the signature's prognostic ability conducted using Gene Expression Omnibus cohorts (GSE215119, GSE190113, and GSE65904), demonstrating consistent survival separation between risk groups.

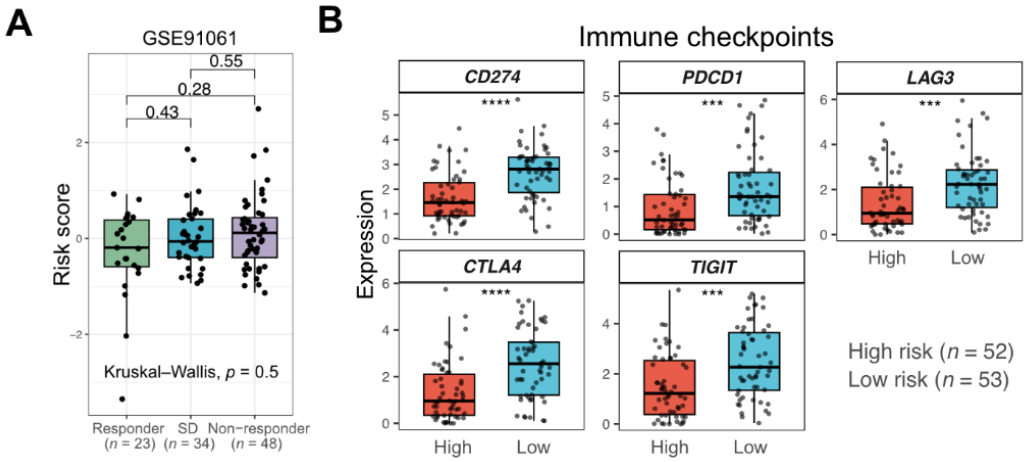


Figure A2. Validation of the autophagy-related risk signature in an anti-PD-1-treated melanoma cohort (GSE91061). (A) Distribution of risk score among patients with different immunotherapy outcomes (responders, stable disease [SD], and non-responders). (B) Comparison of immune checkpoint gene expression between two risk groups. Overall differences among the three groups were evaluated using the Kruskal–Wallis test in A. Other statistical significance was determined by the Wilcoxon rank-sum test in A and B. Notes: $^{*}p < 0.05$; $^{**}p < 0.01$.